Journal of Advanced Research in Fluid Mechanics and Thermal Sciences

Journal homepage:
https://semarakilmu.com.my/journals/index.php/fluid_mechanics_thermal_sciences/index
ISSN: 2289-7879

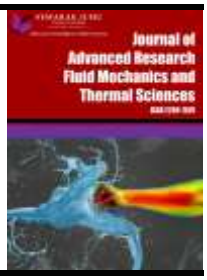

CFD Analysis of the Generic Isolated Gable Roof Stadium: Impact of Opening Direction and Roof Angle for Wind Drift in Badminton

Vignesh Subramani Mahalakshmi[1,*], Nallavan Govindarajan[1], Ramakrishnan Raju[1], Oumar Drame[2]

[1] Department of Sports Technology, Tamil Nadu Physical Education and Spots University, Chennai, India
[2] Fluid Mechanics and Application Laboratory, Cheikh Anta Diop University, Dakar, Senegal

ARTICLE INFO

Article history:
Received 5 April 2024
Received in revised form 10 July 2024
Accepted 19 July 2024
Available online 15 August 2024

Keywords:
Badminton; wind drift; ventilation; gable roof; computational fluid dynamics

ABSTRACT

Badminton is highly influenced by wind drift due to indoor ventilation, which changes the trajectory of the shuttlecock from the actual. To understand the influence of wind drift over different stadium configuration is studied using Computational Fluid Dynamics (CFD). CFD is an essential tool to assess and understand the impact of wind in the building environment for ventilation comforts. Many studies on natural or cross ventilation on the generic model and stadium infrastructure focus only on the ventilation comfort but limitedly on the wind influence like wind drift in badminton. Therefore, this paper presents a detailed study through computational analysis of the isolated generic model with three gable roof slopes ratio and two opening directions. The simulation is performed in a 3D steady Reynolds-Averaged Navier–Stokes (RANS) approach with the SST k–ω model. Validation is carried out with grid sensitivity study by comparing study of a published work with wind tunnel experiment data on a flat roof model. The results show that the gable roof in the longitudinal direction with a 6:12 and 4:12 sloped ratio performed better than a flat roof with a 6% and 13% volume flow rate higher with almost no wind drift near the ground (h=0.02m). The 2:12 sloped gable roof has a higher volume flow rate in both longitudinal and lateral wind flow than the flat roof, with 26% and 37 % higher but a more drifty environment.

1. Introduction

In sports stadium infrastructure, especially in the indoor arena/stadiums natural/cross ventilation is vital due to sustainability and less maintenance than Heat Ventilation and Air-Conditioning (HVAC). There was a unique challenge in designing the ventilation system for a sports stadium; it needed to provide ventilation comfort for the spectators and players without indoor wind disturbance for the sports activity. In badminton, the shuttlecock is used instead of a ball, a lightweight bluff body that will change from the actual trajectory due to indoor wind leading to a colossal setback for elite badminton players. The wind drift is due to natural ventilation caused by wind flow from doors, ventilation openings/windows and the HVAC system [1-6]. The natural/cross ventilation in the

* *Corresponding author.*
E-mail address: emailsmvignesh@gmail.com

https://doi.org/10.37934/arfmts.120.1.5767

building depends on many parameters such as the volume of the building, roof configuration (size and shape), external wind direction and temperature, opening in the building (Size and Inlet-outlet location) and impact of surrounding environments is known from Awbi [7]. There are many studies on an isolated model for cross-ventilation based on the impact of computational parameters, roof geometries and types, leeward and windward opening location and size, symmetrical and asymmetrical opening, and an effect of wind catcher or tower [8-19]. In the case of the stadium, studies are based on ventilation comfort, impact opening types, thermal comfort, pedestrian comfort, pollution dissertation, wind influence around the stadium at different wind directions and impact of the surrounding environment [20-28]. Several studies have been carried out on ventilation comfort in isolated models and sports stadiums, but there has yet to study on badminton wind drift with ventilation comfort [13-24].

A gable roof is the one of the common roof structures used mostly to construct the badminton stadium with cross ventilation. Studies like peak pressure impact and wind-induced loads at different geometry are studied in gable roofs [8,9]. In the case of an inlet-outlet opening across the building, there were symmetrical and unsymmetrical openings, different heights, and different ratios studied in previous studies [12-19]. However, studies have yet to be conducted on the different gable roof configuration in the longitudinal and lateral opening of the model. Therefore, this paper will investigate the impact of the gable roof slope ratio and with opening direction in a generic isolated environment in Computational Fluid Dynamics (CFD). This paper will employ the coupled approach, where the indoor and outdoor wind flow model is simulated simultaneously in the following CFD studies at the same computational domain [29].

The aim of the study is not only to identify the best ventilation comfort roof configuration or opening direction but also the having a minimum wind drift near the ground. For validation purposes, the flat roof with two opposite openings is studied with the same model geometry and wind flow data from the literature on the wind tunnel experiment by Karava *et al.,* [29]. The study will analyze the seven different models, where one is the flat roof validating model [3].

(L X B X H = 0.1 X 0.1 X 0.08 m^2) with an opening in opposite directions at the top of the building at the height 0.06m from the ground to the center of the opening. The gable roof is studied with three different configurations in two opening directions; in total, six gable roofs are subjected to CFD analysis to understand the ventilation and wind drift among them. The horizontal measurement line between the inlet and outlet is to measure the non-dimensional wind velocity for validating with wind tunnel data taken from Karava *et al.,* [29] and to understand the wind flow between the opening (Inlet to outlet) is influencing the indoor environment which leads to a wind drift. The non-dimensional velocity contour is visualized in the vertical plane in the center and at the horizontal plane (h=0.06m) to visualize the wind flow exchange between the opening and the horizontal plane (h=0.02m) for understanding the wind flow pattern and dominating wind drift areas.

2. CFD Simulation

The simulation is carried out with wind tunnel experiment model dimensions by Karava *et al.,* [29] and computational parameters carried out based on Ramponi and Blocken [15] and Perén *et al.,* [18]. The gable roof is designed above the flat roof model at the different slope (rise/run) configurations (Figure 1(a) and Figure 1(b)) to understand the influences wind drift and ventilation [29]. The three different roof configuration models are developed for the analysis at the slope ratio (rise: run) 6:12, 4:12 and 2:12. The wind flow in all roof configurations is studied in longitudinal and lateral opening in the opposite direction to each other at 10% porosity with opening dimensions L X H = 0.046 X 0.018 m2 (Figure 1(c) and Figure 1(d)).

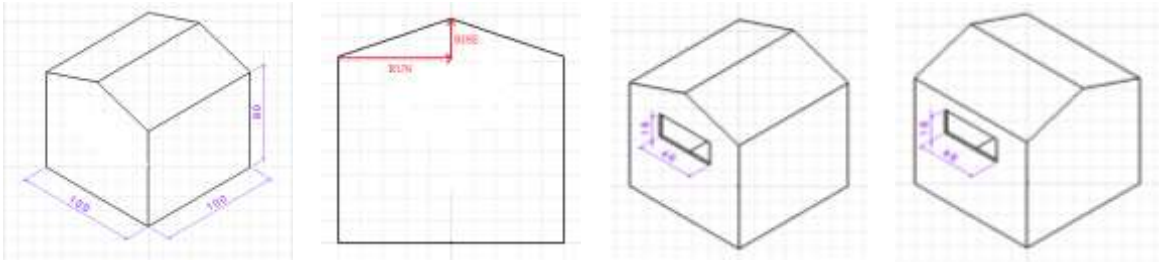

(a) (b) (c) (d)

Fig. 1. (a) Perspective view of the scale down model with dimensions in mm (b) Front view of the model illustrating the run and rise length (c) Perspective view of longitudinal wind flow opening with dimension in mm (d) Perspective view of lateral wind flow opening with dimension in mm

2.1 Domain and Grid Generation

The commercial package ANSYS Fluent user manual is used for grid generation and CFD simulation [30]. The cuboidal domain with a model is constructed in the dimension L X B X H = 1.9m X 1.1m X 0.6m (Figure 2(a)), and the model is located from the inlet plane at three times the height of the model. The structured mesh was generated using the partitioning technique, where the domain is divided into separate volumes, and a fine grid is generated in the model volume. The reference mesh model has 4,31,796 grids cell (Figure 2(b)), and the grid sensitivity will be discussed in subsequent section.

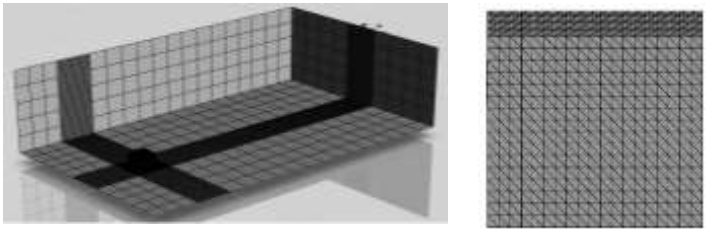

(a) (b)

Fig. 2. Computational grid model (a) Perspective view of grid in building model, ground, side and outlet wall (b) Reference model grid of the side view in longitudinal wind flow opening model

2.2 Boundary Condition and Solver Settings

The front plane of the domain is the inlet, where the Atmospheric Boundary Layer (ABL) velocity profile is enabled based on Karava *et al.,* [29] wind tunnel measurements data is referred from Karava *et al.,* [29,31] and according to the logarithmic law Eq. (1), Where U (y) is the velocity-inlet profile, U* the ABL frictional velocity, Ǩ the von Karman constant, y the height of the domain and y_o the aerodynamics roughness length. For turbulent kinetic energy - k(y), epsilon - ɛ́(y), omega - ω(y), is computed based on the reference from Ramponi and Blocken [16] and Perén *et al.,* [18]. The zero static pressure is maintained in the rear plane of the domain, has a pressure outlet, and a zero-velocity gradient is applied to the side and upper wall of the domain. Based on the literature recommendation in the studies by Ramponi and Blocken [15,16] and Perén *et al.,* [18], the model and ground surface impose the roughness height and roughness constant.

$$U(y) = \frac{U*}{K} \ln\left[\frac{(y+y.)}{y.}\right] \quad (1)$$

The simulation is carried out with the commercial CFD package Fluent. The SST k-ω model and 3D steady RANS equation was solved in a combined manner. The pressure-velocity coupling, interpretation and discretization are all in the second-order scheme with the SIMPLE algorithm is used in the previous studies [16,18]. It was assumed to attain the convergence at the scaled residual leveled and reached a minimum of 10^{-4} for continuity and specific dissipation rate (ω), 10^{-5} for turbulence kinetic energy (k) and 10^{-6} for x, y and z momentum is reliably monitored until 10,000 iterations to reach a stationary solution. The turbulence model for the study is selected based on the literature Ramponi and Blocken [15], where the simulation is compared between different turbulence model to understand the impact of turbulence, where the SST k-ω model, SST k- ε model, Sk- ε model, Rk- ε model, RNG k- ε model, Sk-ω model and RSM model. Among all turbulence model, SST k-ω model shows the best performance for a generic isolated cross-ventilation CFD simulation.

2.3 Grid Sensitivity and Comparison with Wind Tunnel Data

The grid sensitivity analysis is carried out on the flat where the non-dimensional velocity across the horizontal line between the opening (Figure 3(a)) is compared for the reference (4,31,796 cells), course (2,09,796 cells) and fine (6,92,521 cells) mesh model. From the observation, it was found that the course mesh has a huge drop in the non-dimensional velocity (Figure 4(a)) from the windward opening to the middle of the model. There is no significant difference between the reference mesh and the fine mesh which concludes that the non-dimensional velocity parameter (Figure 4(a)) becomes insensitive to an increase in the number of grids. To save the iteration timing and computational power demand, it is optimizing to select the reference mesh for the rest of the roof models. The reference mesh results gave a good argument with Karava *et al.,* [29] experiment data based on their study (Figure 4(b)) from the inlet opening to the middle where the experiment data is lacks towards the outlet opening of the model due to the effect of reflecting and shading, which is similar to previous studies [18,29]. The contour of non-dimensional velocity is measured in the center in a vertical plane (Figure 5(a)) and the horizontal plane at h = 0.06m (Figure 5(b)) to understand the wind flow exchange between the opening. The wind drift area is visualized in the horizontal plane at h=0.02m (Figure 5(c)), and the ventilation flow rate will be computed to understand the impact of the roof slope ratio's.

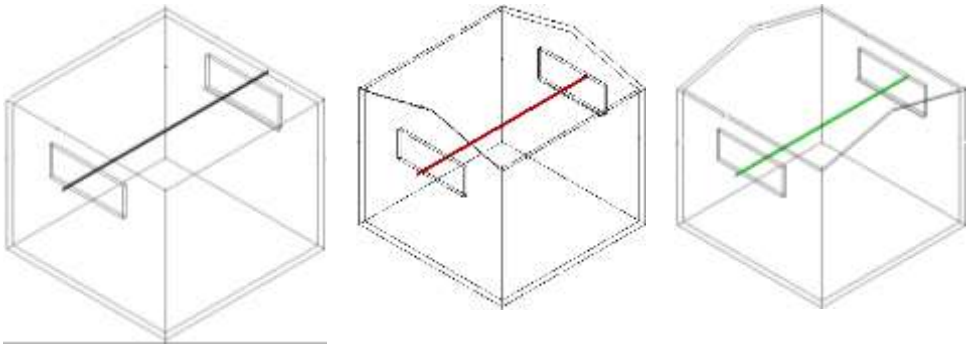

(a) (b) (c)

Fig. 3. Horizontal line between the opening center for measuring the U/U_{ref} (a) Flat roof (b) Gable roof in longitudinal wind flow opening direction (c) Gable roof in Lateral wind flow opening direction

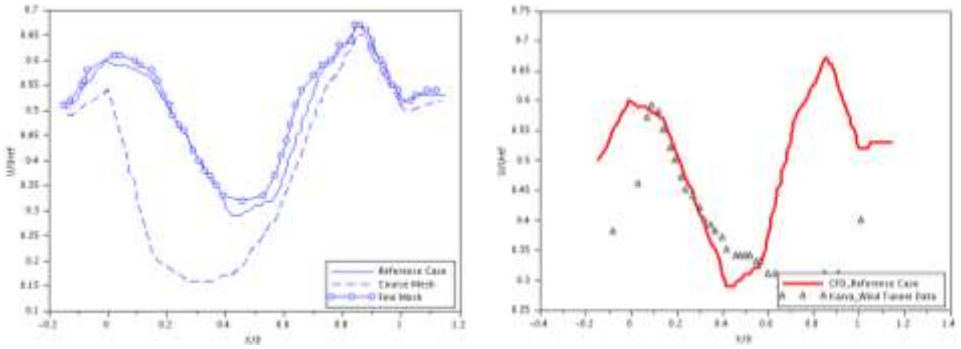

(a) (b)

Fig. 4. (a) Comparison of impact of grid sensitivity in mean wind velocity (U/U_{ref}) between the opening along the horizontal line in flat roof. (b) Comparison of numerical data of reference mesh and wind tunnel data of mean wind velocity between the opening along the horizontal line in flat roof

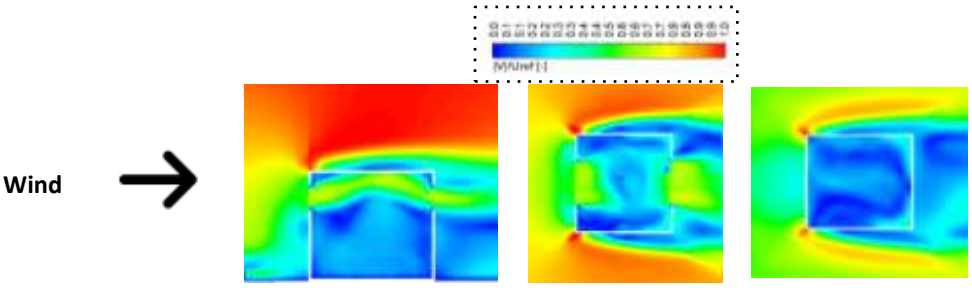

(a) (b) (c)

Fig. 5. Flat roof non-dimensional velocity ($|V|/U_{ref}$) contours (a) Vertical plane at center of the model (b). Horizontal plane at height = 0.06m from the ground of the model and (c). Horizontal plane at height = 0.02m from the ground of the model

3. Impact of Gable Roof Configuration and Wind Flow

To understand the impact of the gable roof configuration on wind drift for badminton stadium or arena, the analysis is done through non-dimensional contour (Figure 5 to Figure 11), Velocity vector of horizontal plane at 0.02m (Figure 12) and mean non-dimensional velocity in a plane (Table 1). The three configurations in a longitudinal and lateral wind flow at the different slope ratio (rise:run) 6:12, 4:12 and 2:12. In all three cases the inlet to outlet opening distance, location and size maintain to be the same. The velocity contour in the center vertical plane and horizontal plane (h=0.06m and 0.02m) (Figure 6 to Figure 11), Velocity vector at horizontal plane (Figure 12), non-dimensional velocity in the horizontal line (Figure 3(b) and Figure 3(c)) between the opening (Figure 13) and volume flow rate (Figure 14) will be analyzed to compare the gable roof slope and opening direction impact.

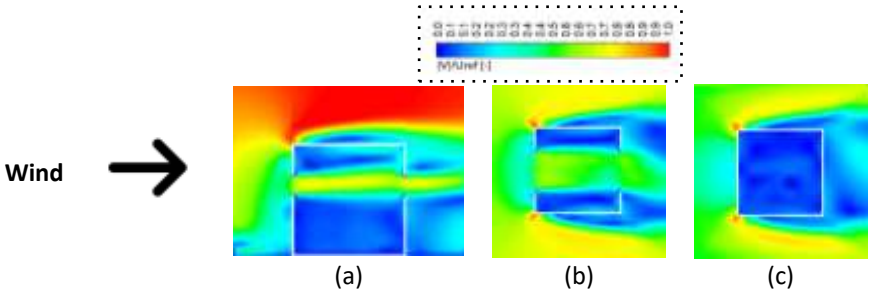

Fig. 6. Gable roof [6:12] non-dimensional ($|V|/U_{ref}$) contours - longitudinal wind direction (a) Vertical plane at center of the model (b). Horizontal plane at height = 0.06m from the ground of the model and (c). Horizontal plane at height = 0.02m from the ground of the model

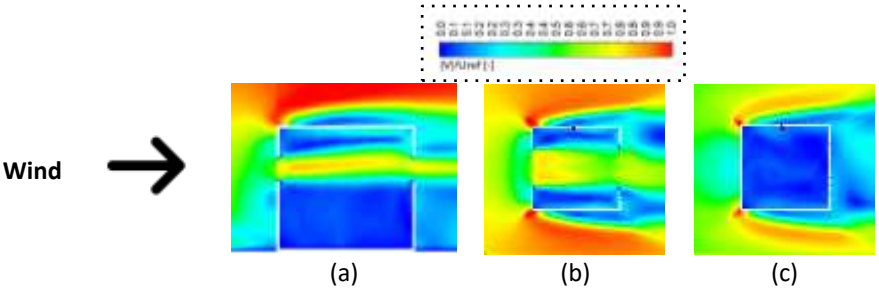

Fig. 7. Gable roof [4:12] non-dimensional ($|V|/U_{ref}$) contours - longitudinal wind direction (a) Vertical plane at center of the model (b). Horizontal plane at height = 0.06m from the ground of the model and (c). Horizontal plane at height = 0.02m from the ground of the model

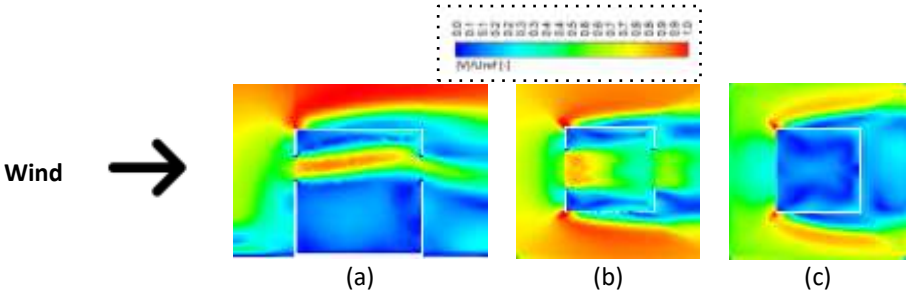

Fig. 8. Gable roof [2:12] non-dimensional ($|V|/U_{ref}$) contours - longitudinal wind direction (a) Vertical plane at center of the model (b). Horizontal plane at height = 0.06m from the ground of the model and (c). Horizontal plane at height = 0.02m from the ground of the model

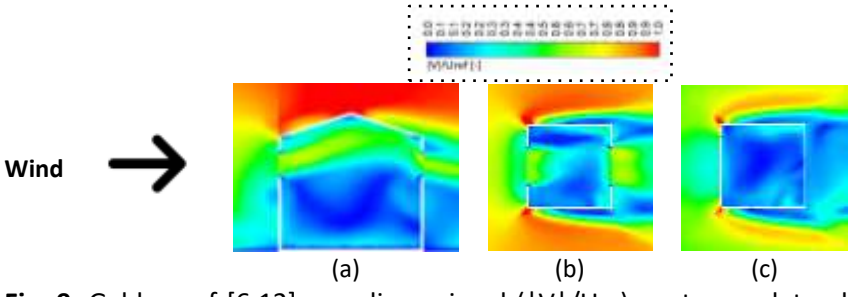

Fig. 9. Gable roof [6:12] non-dimensional ($|V|/U_{ref}$) contours - lateral wind direction (a) Vertical plane at center of the model (b). Horizontal plane at height = 0.06m from the ground of the model and (c). Horizontal plane at height = 0.02m from the ground of the model

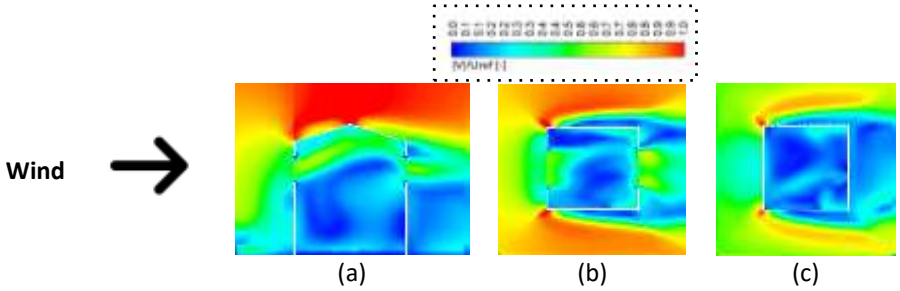

Fig. 10. Gable roof [4:12] non-dimensional ($|V|/U_{ref}$) contours - lateral wind direction (a) Vertical plane at center of the model (b). Horizontal plane at height = 0.06m from the ground of the model and (c). Horizontal plane at height = 0.02m from the ground of the model

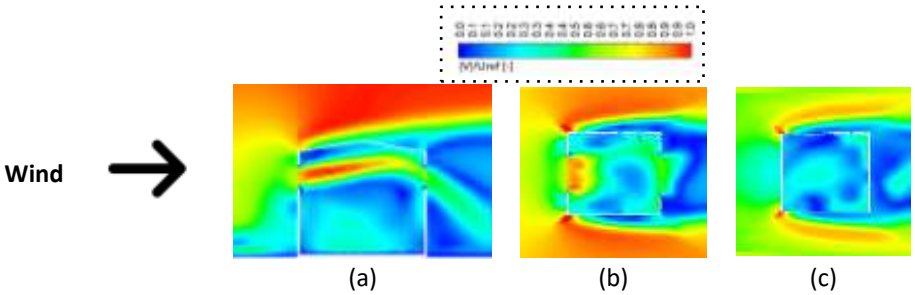

Fig. 11. Gable roof [2:12] non-dimensional ($|V|/U_{ref}$) contours - lateral wind direction (a) Vertical plane at center of the model (b). Horizontal plane at height = 0.06m from the ground of the model and (c). Horizontal plane at height = 0.02m from the ground of the model

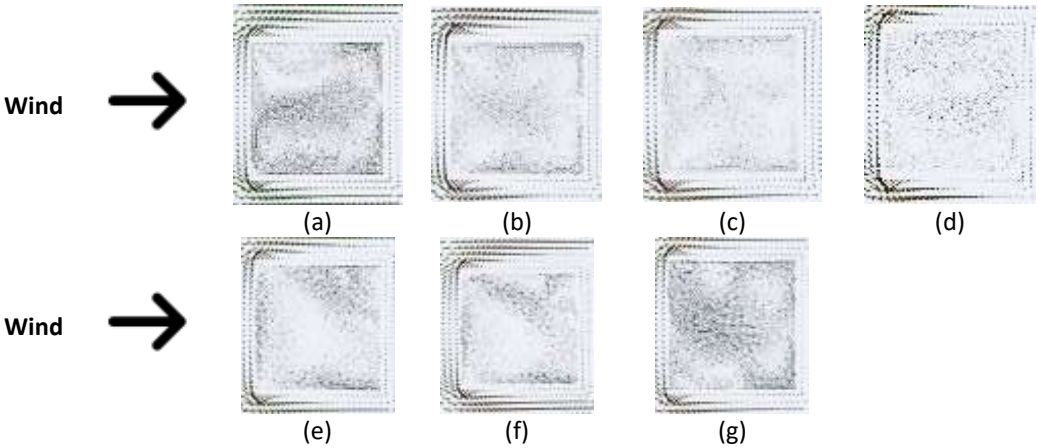

Fig. 12. Gable roof velocity vector at the horizontal plane at height = 0.02 m from the ground of the model. (a)Flat roof, Longitudinal wind direction (b). 6:12 (c). 4:12 and (d). 2:12 and Lateral wind direction (e). 6:12 (f) 4:12 and (g)

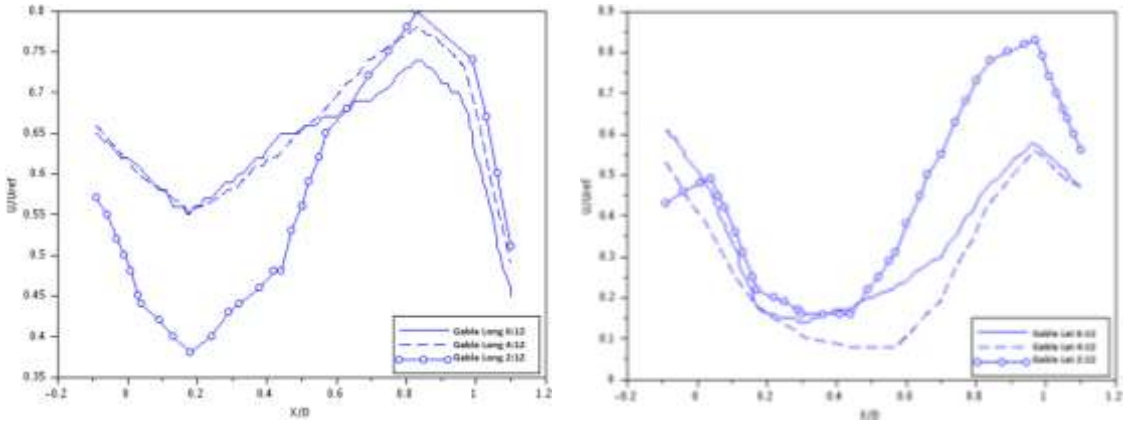

(a) (b)

Fig. 13. Impact of roof configuration (a) U/U_{ref} along the horizontal line in gable roof in longitudinal flow direction for different slope ratio (b) U/U_{ref} along the horizontal line in gable roof in lateral flow direction for different slope ratio

Table 1 gives more insight into different gable roof configurations where the mean U/U_{ref} in the vertical (center) and horizontal plane (h=0.06m) between the opening is studied for the exchange of wind flow. The horizontal plane (h=0.02m) mean U/U_{ref} gives insights into the wind drift. In longitudinal wind flow, the 2:12 configuration has a huge drop in the non-dimensional velocity (Figure 13(a)) from the inlet opening to almost the middle of the model due to deviation of flow toward the roof compared to 6:12 and 4:12, where there no huge change except near to the outlet opening. In 6:12 and 4:12, the wind flow exchanged between the opening without deflection from the roof (Figure 6(a) and Figure 7(a)) led to less wind drift near the ground (Table 1), but 2:12 had an increase in dirty area (Figure 8(a)) (Table 1) due to the flow deflection near the outlet opening. All three-roof configuration in lateral wind flow deviates upward to the roof (Figure 9(a), Figure 10(a) and Figure 11(a)), causing a drifty environment near the ground that is almost the same or more than a flat roof. The 2:12 possess a peak mean U/U_{ref} (Table 1) in the horizontal plane (h=0.02m), leading to a more drifty area (Figure 11(c)) than any other roof configuration. Altogether, the longitudinal wind flow performs better than a lateral wind flow with a less dirty region (Table 1). For all wind direction and roof configuration, the velocity vector is visualized in the horizontal plane at 0.02m from the ground to understand the no wind drift area. In 6:12 and 4:12 configurations in longitudinal wind flow (Figure 6(c) and Figure 7(c)) seems to have a better performance which possess a shallow drifty area compared to other configurations including the flat roof.

Table 1
Mean non-dimensional velocity in different plane area at longitudinal and lateral wind flow in gable roof

Model Case	Vertical plane inside the model at center	Horizontal plane inside the mode at h=0.06m	Vertical plane inside the mode at h=0.02m
Reference Case	0.24	0.28	0.12
6:12_Longitudinal	0.23	0.37	0.06
4:12_Longitudinal	0.22	0.39	0.05
2:12_Longitudinal	0.26	0.41	0.10
6:12_Lateral	0.23	0.22	0.10
4:12_Lateral	0.21	0.21	0.12
2:12_Lateral	0.31	0.36	0.20

From Figure 14, We can conclude that the volume flow rate for the gable roof 2:12 in lateral wind flow is the highest among all other roofs, with an increase of 37% compared to the flat roofs. In

longitudinal wind flow, 2:12 is highest among 4:12 and 6:12, with an increase of 26% compared to the flat roof. The 4:12 in longitudinal opening direction has a better volume flow rate with a low wind drift area compared to other configurations, with an increase of 13% comparative to the flat roof. Comparing 6:12 and 4:12 in lateral wind flow has no significant difference in volume flow rate but decrease by almost 10% compared to a flat roof (Figure 14). It can be noticed that the lowest slope ratio of the roof will impact largely in the volume flow rate, both a flow direction lower slope configuration gains high volume flow rate.

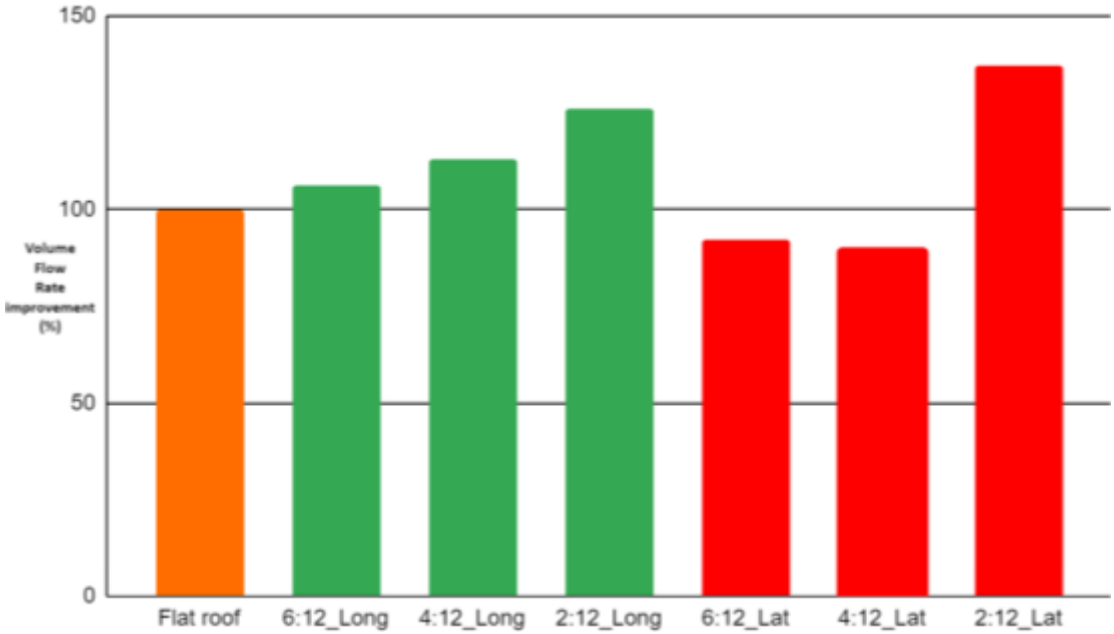

Fig. 14. Influence of roof slope ratio with opening flow direction for gable roof on volume flow rate improvement in percentage comparing with flat roof

4. Conclusion

The above study result is to understand the influence of the gable roof configuration with some limitation. CFD simulation is carried isothermal conditions with a flat roof and three different slopes of a gable roof (6:12, 4:12 and 2:12) in an isolated condition without an internal layout with cross ventilation opposite opening in longitudinal and lateral wind flow direction to understand the dominance of the wind drift (wind velocity near ground h=0.02m) in badminton stadium.

The following conclusion has been obtained from this study

i. The six types of CAD model are developed, where two types of roof type and three types of sloped roof ratio (Figure 1) for the CFD simulation to understand the wind drift and ventilation for the development of badminton stadium.
ii. The grid sensitivity analysis (Figure 2 and Figure 4(a)) is carried out in the flat roof, where the reference case selected for the analysis which perform will computationally with acceptable computational time and resource.
iii. Turbulence model and other computational parameter is selected based on the best practice provided in the literature for the isolated building cross ventilation analysis. Based on the literature recommendation, SST k-ω model perform well to predict the ventilation performance and validated well with experimental data (Figure 4(b)).
iv. The non-dimensional velocity contour at vertical plane at the centre and vertical plane at height 0.06m and 0.02m from ground (Figure 5 to Figure 11); Velocity vector at the

horizontal plane at height 0.02m from the ground (Figure 12); U/U_{ref} is measured in the horizontal line in the centre of the opening (Figure 13); Mean non-dimensional velocity at both vertical plane at height 0.06m and 0.02m from ground (Table 1) and Volume flow rate compared with flat roof (Figure 14) is analysed for all the roof configuration to understand the wind drift and ventilation.

v. In longitudinal wind flow direction, the gable roof with slope ratio 6:12 and 4:12 performs better (Figure 6(c) and Figure 7(c)) with higher volume flow rate than a flat roof (Figure 14) and lower wind drift compared to 2:12, even though it has higher volume flow rate (Figure 14) but has a huge drifty environment (Figure 8(c)).

vi. In longitudinal wind flow direction, a 4:12 sloped roof is recommended because 6:12 has a lower volume flow rate (Figure 14) comparatively, but both have the same lower drifty environment.

vii. In the lateral direction, 6:12 and 4:12 sloped roofs have no significant change in the drift environment compared to flat roof (Table 1) but have decreased to 10% in volume flow rate (Figure 14).

viii. The 2:12 sloped roof in lateral wind direction possesses a more drifty environment (Table 1) with a higher volume flow rate among all roof configurations (Figure 14).

ix. The CFD simulation is carried out in the isolated condition, there is need of analysis with surrounding environment for the better understanding in the wind drift and ventilation.

x. The CFD analysis is carried in the isothermal condition and steady state, where this analysis demand the actual scenario with environmental and weather condition for the more insights to balance both wind drift and ventilation in the Badminton stadium.

xi. The real-time case study will be carried out with CFD and experiment in the Badminton stadium in the future research for more progress in development of lower the wind drift court area with optimized ventilation.

Acknowledgement
The authors would like to thank a Department of Sports Technology, Tamil Nadu Physical Education and Sports University for providing a Laboratory resource for this research. This research was not funded by any grant.

References

[1] AFP. "Air-con controversy not cool for badminton." *BangkokPost*. August 15, 2013.
[2] AFP. "Air-conditioning row an uncool distraction at badminton world championships." *South China Post*. August 16, 2013.
[3] AFP. "No evidence of badminton aircon cheating: official." *Business Standard*. September 26, 2014.
[4] Klug, Foster. "Get the drift? Badminton players face indoor winds in Rio." *USA Today*. August 13, 2016.
[5] Klug, Foster. "Air conditioning 'drifts' pose problems for Olympic badminton players." *The Star*. August 13, 2016.
[6] Rayan, Stan. "Wind a worry for P.V. Sindhu." *Sportstar*. August 18, 2018.
[7] Awbi, Hazim B. *Ventilation systems: design and performance*. Routledge, 2007. https://doi.org/10.4324/9780203936894
[8] Quan, Yong, Yukio Tamura, and Masahiro Matsui. "Mean wind pressure coefficients on surfaces of gable-roofed low-rise buildings." *Advances in Structural Engineering* 10, no. 3 (2007): 259-271. https://doi.org/10.1260/136943307781422253
[9] Kindangen, J., G. Krauss, and P. Depecker. "Effects of roof shapes on wind-induced air motion inside buildings." *Building and Environment* 32, no. 1 (1997): 1-11. https://doi.org/10.1016/S0360-1323(96)00021-2
[10] Kindangen, Jefrey I. "Window and roof configurations for comfort ventilation." *Building Research & Information* 25, no. 4 (1997): 218-225. https://doi.org/10.1080/096132197370345
[11] Stathopoulos, Theodore, and Abdol Rasool Mohammadian. "Modelling of wind pressures on monoslope roofs." *Engineering Structures* 13, no. 3 (1991): 281-292. https://doi.org/10.1016/0141-0296(91)90039-F

[12] Prasad, Deepak, Tuputa Uliate, and M. Rafiuddin Ahmed. "Wind loads on low-rise building models with different roof configurations." *International Journal of Fluid Mechanics Research* 36, no. 3 (2009). https://doi.org/10.1615/InterJFluidMechRes.v36.i3.30
[13] Hu, Cheng-Hu, Masaaki Ohba, and Ryuichiro Yoshie. "CFD modelling of unsteady cross ventilation flows using LES." *Journal of Wind Engineering and Industrial Aerodynamics* 96, no. 10-11 (2008): 1692-1706. https://doi.org/10.1016/j.jweia.2008.02.031
[14] Meroney, Robert N. "CFD prediction of airflow in buildings for natural ventilation." In *Proceedings of the Eleventh Americas Conference on Wind Engineering*, Puerto Rico. 2009.
[15] Ramponi, Rubina, and Bert Blocken. "CFD simulation of cross-ventilation flow for different isolated building configurations: validation with wind tunnel measurements and analysis of physical and numerical diffusion effects." *Journal of Wind Engineering and Industrial Aerodynamics* 104 (2012): 408-418. https://doi.org/10.1016/j.jweia.2012.02.005
[16] Ramponi, Rubina, and Bert Blocken. "CFD simulation of cross-ventilation for a generic isolated building: Impact of computational parameters." *Building and Environment* 53 (2012): 34-48. https://doi.org/10.1016/j.buildenv.2012.01.004
[17] Chu, Chia-Ren, and Bo-Fan Chiang. "Wind-driven cross ventilation in long buildings." *Building and Environment* 80 (2014): 150-158. https://doi.org/10.1016/j.buildenv.2014.05.017
[18] Perén, J. I., T. Van Hooff, Brenda Chaves Coelho Leite, and Bert Blocken. "CFD analysis of cross-ventilation of a generic isolated building with asymmetric opening positions: Impact of roof angle and opening location." *Building and Environment* 85 (2015): 263-276. https://doi.org/10.1016/j.buildenv.2014.12.007
[19] Kato, Shinsuke, Shuzo Murakami, Akashi Mochida, Shin-ichi Akabayashi, and Yoshihide Tominaga. "Velocity-pressure field of cross ventilation with open windows analyzed by wind tunnel and numerical simulation." *Journal of Wind Engineering and Industrial Aerodynamics* 44, no. 1-3 (1992): 2575-2586. https://doi.org/10.1016/0167-6105(92)90049-G
[20] Van Hooff, T., and Bert Blocken. "Coupled urban wind flow and indoor natural ventilation modelling on a high-resolution grid: A case study for the Amsterdam ArenA stadium." *Environmental Modelling & Software* 25, no. 1 (2010): 51-65. https://doi.org/10.1016/j.envsoft.2009.07.008
[21] Van Hooff, Twan, and Bert Blocken. "On the effect of wind direction and urban surroundings on natural ventilation of a large semi-enclosed stadium." *Computers & Fluids* 39, no. 7 (2010): 1146-1155. https://doi.org/10.1016/j.compfluid.2010.02.004
[22] Van Hooff, Twan, and Bert Blocken. "Full-scale measurements of indoor environmental conditions and natural ventilation in a large semi-enclosed stadium: possibilities and limitations for CFD validation." *Journal of Wind Engineering and Industrial Aerodynamics* 104 (2012): 330-341. https://doi.org/10.1016/j.jweia.2012.02.009
[23] Van Hooff, T., and B. Blocken. "CFD evaluation of natural ventilation of indoor environments by the concentration decay method: CO_2 gas dispersion from a semi-enclosed stadium." *Building and Environment* 61 (2013): 1-17. https://doi.org/10.1016/j.buildenv.2012.11.021
[24] Chen, Lei, and Yangluxi Li. "Effects of different auditorium forms on ventilation in a football stadium." *Indoor and Built Environment* 29, no. 8 (2020): 1070-1086. https://doi.org/10.1177/1420326X19873132
[25] Van Hooff, Twan, Bert Blocken, and M. Van Harten. "3D CFD simulations of wind flow and wind-driven rain shelter in sports stadia: influence of stadium geometry." *Building and Environment* 46, no. 1 (2011): 22-37. https://doi.org/10.1016/j.buildenv.2010.06.013
[26] Mei, Weijun, and Ming Qu. "Evaluation and analysis of wind flow for a football stadium." *Procedia Engineering* 145 (2016): 774-781. https://doi.org/10.1016/j.proeng.2016.04.101
[27] Sofotasiou, Polytimi, Benjamin Richard Hughes, and John Kaiser Calautit. "Qatar 2022: Facing the FIFA World Cup climatic and legacy challenges." *Sustainable Cities and Society* 14 (2015): 16-30. https://doi.org/10.1016/j.scs.2014.07.007
[28] Sofotasiou, P., B. R. Hughes, and J. K. Calautit. "Thermal performance evaluation of semi-outdoor sport stadia: A case study of the upcoming 2022 FIFA World Cup in Qatar." *Proceedings of the ASHRAE Hellenic* (2014).
[29] Karava, Panagiota, Ted Stathopoulos, and A. K. Athienitis. "Airflow assessment in cross-ventilated buildings with operable façade elements." *Building and Environment* 46, no. 1 (2011): 266-279. https://doi.org/10.1016/j.buildenv.2010.07.022
[30] ANSYS, Ins. "ANSYS fluent 12.0 User's Guide." *New Hampshire: Ansys Inc* (2009).
[31] Karava, Panagiota, Ted Stathopoulos, and Andreas K. Athienitis. "Wind-induced natural ventilation analysis." *Solar Energy* 81, no. 1 (2007): 20-30. https://doi.org/10.1016/j.solener.2006.06.013